Ultrafine nickel nanoparticles modified reduced graphene oxide as efficient non-platinum catalysts for methanol oxidation

Hongmei Sun,[a,b] Jun Liu,[a] Zhenfei Tian,[a] Yixing Ye,[a] and Changhao Liang* [a,b]

[a] Key Laboratory of Materials Physics and Anhui Key Laboratory of Nanomaterials and Nanotechnology, Institute of Solid State Physics, Hefei Institutes of Physical Science, Chinese Academy of Sciences, Hefei 230031, China.

[b] Department of Materials Science and Engineering, University of Science and Technology of China, Hefei 230026,China.

Highlights

- Ultrafine nickel nanoparticles modified reduced graphene oxide (Ni/rGO) catalysts were prepared by liquid phase laser ablation (LPLA) and in situ reducing process.
- The growth and aggregation of Ni colloids were restricted by graphene oxide during LPLA.
- Ultrafine nickel nanoparticles with the size ranging from 1.5 to 3.6 nm were embedded into reduced graphene oxide.
- Ni/rGO exhibited the ultrahigh catalytic mass activity of 1600 mA/mg, methanol saturation concentration (4 M), and long stability (1020 mA/mg after 1000 cycles).

Abstract

Synthesis of low-cost, highly-active and durable non-platinum metal catalysts for methanol oxidation reaction (MOR) is always full of challenge. Here, Ni nanoparticles modified reduced graphene oxide (Ni/rGO) as an efficient non-platinum catalyst were synthesized by laser ablation of Ni target in graphene oxide (GO) solution and the following in situ reduction process. It found that GO played an important role to restrict the growth and aggregation of ultrafine nickel colloids (< 5 nm) in the process of laser ablation. The resulting Ni/rGO catalyst showed advantageous in active sites and charge transport resulting from the small particle size, uniform dispersion and electronic effect arising from the electron interactions between reduced graphene oxide (rGO) and Ni. The obtained Ni/rGO exhibited the ultrahigh catalytic mass activity of 1600 mA/mg, methanol saturation concentration (4 M), which was superior to that of the reported Ni-based catalysts. Remarkably the mass activities of Ni/rGO before and after 1000 cycles exceed that of the commercial Pt/C catalyst, indicating excellent catalytic activity and stability.

1：Introduction

Direct methanol fuel cells (DMFCs) have attracted much attention due to a variety of advantages, such as high energy density, low operating temperature and facile electrode catalytic reactions.[1] [2] As the DMFC anode catalyst, traditional noble metal, especially Pt and Pt-based alloy[3] [4] are extensively used for electrocatalytic oxidation of methanol (MOR), whereas their high cost and poor stability hinder the practical applications . Therefore, exploring non-platinum metals with high activity and long stability has been one of the research hotspots in MOR. Among non-platinum metal catalysts, nickel-based catalysts are considered as the most promising candidates due to the high catalytic activity and low cost of nickel. [5] [6] Much ongoing efforts have been devoted to fabricating nickel-based catalysts in recent years,[7] such as nickel nanoparticles modified polymer composites,[8] flower-like NiO,[9] porous NiO film,[10] astrocyte-network Ni-P-O compound.[11]

In order to obtain highly efficient MOR electrocatalysts, downsizing nickel composites to enhance the Ni utilization efficiency is an effective method.[10] For example, Knez[12] synthesized different size of NiO NPs uniform dispersion on oxygen functionalized carbon nanotubes (CNTs) by atomic layer deposition, and found the mass activity of NiO with the size of 4.9 nm showed 2 times than the size of 6.5 nm. Wang[13] found small size of Ni nanoparticles resulted in weaker adsorption of reaction intermediates on catalysts surface to affect the activity and stability. Another strategy is use appropriate supports to improve dispersion of Ni nanoparticles. [14] [15] [12]Guo and co-workers[2] used SiC and CNT to impede nickel composites into larger aggregated nanoparticles during the thermal treatment process and confirmed the aggregation of Ni particles will decrease the electron transfer rate. Graphene has been widely used as substrate for the electrochemical catalysts because of its high surface area and excellent electrical conductivity.[16] [17] The inherent properties of graphene not only facilitate electron transfer [18] but also stabilize metal nanocatalysts to prevent severe aggregation. [20] According to the previous reports, nickel nanoparticles modified graphene are commonly synthesized by co-reduction of nickel salt and graphene oxide[21] or the reduction of nickel salt in the presence of graphene[22], thermal decomposition of precursors[23] and electrochemical deposition[7]. However, the large size (average size >7 nm) and the aggregation of synthesized Ni nanoparticles in the process of preparation

preclude catalytic performance. Therefore, developing effective methods to prepare ultrafine nickel uniformly dispersed on graphene is our purpose.

In previous studies, we demonstrated that liquid phase laser ablation (LPLA) is a unique technique to synthesize ultrafine and well-dispersed NPs because of the extreme condition and subsequent quenching process. [24] [25] Here, we fabricated nickel nanoparticles modified reduced graphene oxide (Ni/rGO) by laser ablation of Ni target in graphene oxide (GO) solution and the following in-situ reduction. The ultrafine NiO_x colloids (<5 nm) generated by the LPLA technique were uniformly decorated on the surface of GO and maintained the original size in the following reduction. The obtained Ni/rGO had the small size ranging from 1.5 nm to 3.6 nm of Ni nanoparticles embedded on rGO without aggregation, which is the smallest in the previous reports. The as-obtained Ni/rGO catalysts showed excellent electrocatalytic performance for methanol oxidation.

2 Experimental sections

Chemical Reagents and Materials

All chemicals used in this experiment were analytical grade and applied without further purification. Graphite powder was purchased from Tianjin Guangfu Fine Chemical Research Institute. GO (TEM image and XRD in Figure S1) was fabricated according to a modified Hummers method.[26] [27] Hydrazine hydrate was purchased from Aladdin Industrial Corporation (Shanghai, China). The commercial Pt/C catalyst (20 wt % Pt on Vulcan XC72R carbon) was purchased from Johnson Matthey. Double-distilled water (resistance >18 MΩ cm^{-1}) was used throughout all experiments.

Preparation of nickel nanoparticles modified reduced graphene oxide

Ni/rGO were fabricated by liquid phase laser ablation (LPLA) technique as shown in Scheme 1, the nickel target (99.99% in purity) was fixed in a vessel filled with 15 mL 0.01 M GO solution and ablated for 60 min by a Nd:YAG laser with wavelength of 1064 nm, pulse duration of 10 ns and per pulse laser energy of 60 mJ. After ablation to obtain brown flocculent precipitates(Figure S2b), hydrazine hydrate (0.2 ml) was then added to the above solution and kept at room temperature for 20 h. The resultant black solid (Figure S2c) was collected by centrifugation and washed with deionized water until the solution remained neutral. The final products were obtained by freeze drying.

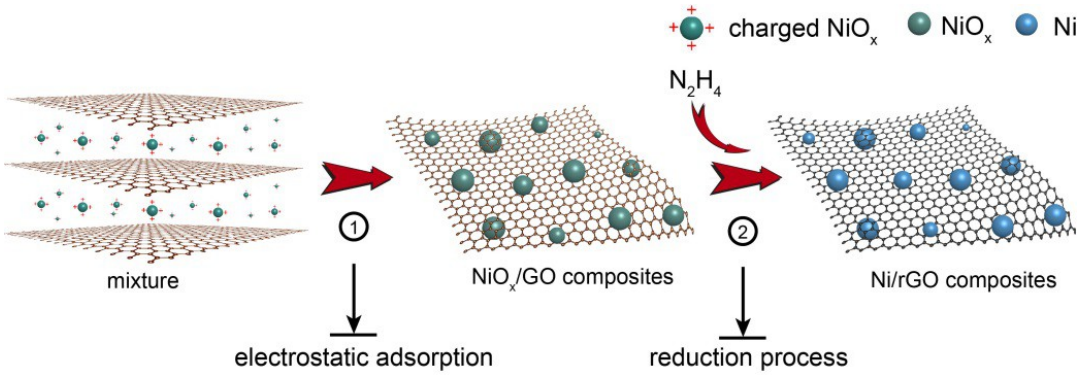

Scheme 1. Schematic illustration of the formation of Ni/rGO

Materials characterization

A transmission electron microscopy (TEM) system (FEI Tecnai G2 F20) with a 200 kV acceleration voltage was used to obtain the structural information of the products and element distribution. X-ray diffraction (XRD) analysis of the collected powder products was performed by using a Philips X'Pert system with Cu-Kα radiated (λ = 1.5419 Å). The surface chemical states were analysed by X-ray photoelectron spectroscopy (XPS, Thermo ESCACLB 250). The Ni content of the samples was measured by an inductively coupled plasma optical emission spectrometer (ICP-OES, Optima 7300 DV, America).

Electrochemical Measurements

Electrochemical measurements were performed on Zahner electrochemical workstation (Germany) using three-electrode systems at room temperature. The reference and counter electrodes were Ag/AgCl (3M KCl) electrode and Pt foil respectively, and the working electrode was prepared through "drop-casting" method, namely, after polishing and washing the glass carbon electrode (GCE), 10 μL as-prepared Ni/rGO composites dispersion was pipetted onto the treated GCE. The concentrations of nickel were obtained through ICP measurement and the total mass of the Ni was 0.75 μg. After drying the electrode in ambient environment for 12 h, 10 μL Nafion solution were following dropped onto these electrodes and dried for another 4 h. Cyclic voltammetry (CV) were conducted in 1 M KOH solution with different concentrations of CH_3OH at scan rates of 50 mV/s. Chronoamperometry (CA) and cycling stability were conducted in 1 M KOH with 1 M CH_3OH to assess the stability of Ni/rGO catalysts. The mass activity of Ni/rGO, which was defined as the peak current per amount of Ni loading, was commonly adopted for evaluating their electrocatalytic performances. For comparison, the commercial Pt/C electrodes

were prepared by the same method.

3: Results

The general formation mechanism of Ni/rGO catalysts in our method involved two key steps: (i) as pulse laser ablating on the interface between Ni target and GO solution, a plasma plume containing Ni species (including atoms, ions, and radicals) was produced. Subsequent ultrasonic and adiabatic expansion of the plume region formed small positive charged NiO_x with high activity and reactivity. These positive charged NiO_x clusters were quickly bound by these adjacent negative charged functional groups on the surface of the GO to form NiO_x-GO composites through electrostatic force. [28] [29] TEM of NiO_x-GO (Figure 1a and Figure 1b) confirmed that plenty of fine grain of NiO_x colloids (< 5 nm) were anchored on GO. While other nickel colloids not captured by GO grew into spherical nanoparticles through oriented aggregation and Oswald ripening (Figure 1c). XRD image of NiO_x-GO (Figure 1d) indicated that the NiO_x-GO colloid solution actually consisted of NiO and fcc Ni, which was confirmed by other related reports.[30] (ii) After reduction of hydrazine hydrate, the strong reducing ability of hydrazine hydrate simultaneously reduced GO and NiO_x according to the following reaction.[31] After reduction of hydrazine hydrate, the diffraction peaks of NiO (Figure 1d) were disappeared indicating NiO nanoparticles were reduced to metal Ni. The diffraction peaks at 44.48°, 51.83° and 76.35° can be indexed as the (111), (200), and (220) planes of fcc Ni (JCPDS No.01-087-0712) respectively.

$$Ni^{2+} + 3N_2H_4 = [Ni(N_2H_4)_3]^{2+} \quad (1)$$

$$2[Ni(N_2H_4)_3]^{2+} + 4OH^- = 2Ni + N_2 + 4H_2O + 5N_2H_4 \quad (2)$$

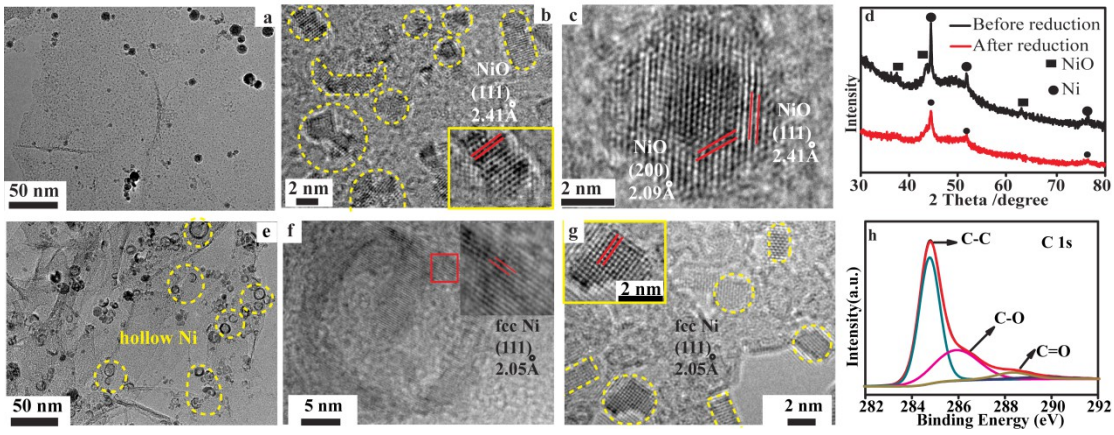

Figure 1. (a) Low-magnification TEM of NiO_x-GO. (b) HR-TEM images of ultrafine NiO_x on

graphene oxide. (c) HR-TEM images of large NiO_x nanoparticles. (d) XRD spectra of before and after reduction of hydrazine hydrate. (e) Low-magnification TEM of Ni/rGO. (f) HR-TEM images of hollow Ni nanoparticles. (g) HR-TEM images of ultrafine Ni nanoparticles embedded into rGO. (h) C1s XPS spectra of Ni/rGO.

TEM images of the prepared Ni/rGO are shown in Figure 1e-g. As seen from TEM images (Figure 1e), Most of the solid NiO nanoparticles converted to the hollow nanoparticles, confirmed the above reaction mechanism. According to the previous reports, hollow structures can enhance catalytic active sites and improve mass transfer as compare to the common solid structures.[32] Its corresponding size distribution histograms (Figure s3a) and HRTEM image (Figure 1b) further reveal that these nanoparticles with average particles size of 7 nm have a lattice spacing of 2.05 Å, which corresponds to the (111) planes of fcc Ni. In the HR-TEM images of rGO (Figure 1f), large quantities of Ni nanoparticles are embedded into rGO, which also acted as bridges to connect the Ni NPs, thereby enhancing the overall electron transfer capability.[33] The corresponding size distribution histograms (Figure S3b) show the size range from 1.5 to 3.6 nm. The formation of the ultrafine Ni NPs indicate that the strong anchoring effect of rGO limit the growth of Ni NPs and prevent its agglomeration. Meanwhile, those Ni nanoparticles on rGO sheets act as spacers to prevent graphene from stacking. Therefore, the rGO nanosheets play an important role in limiting the growth of Ni NPs.

Elemental composition and valence state on the surface of Ni/rGO were further confirmed by XPS, as shown in Figure 1f. High-resolution C1s spectrum of Ni/rGO shows three main peaks correspond to carbon atoms with different oxidation states. These peaks located at the binding energies of 284.5, 286.6 and 288.4 eV are assigned to C-C in aromatic rings, C-O (hydroxyl and 1,2-epoxide functionalities), C=O (carboxyl and ketone functionalities) groups, respectively. [34] [35] Compared with the XPS spectra of GO (Figure S4), an obvious decrease in the intensity of oxygen-containing functional groups indicates that an effective reduction reaction of GO happened after adding hydrazine hydrate. In Ni $2p_{3/2}$ spectrum (Figure S5), a peak located at 852.0 eV corresponds to Ni^0, while another peak at 855.8 eV is ascribed to NiO, indicating the surface of Ni are mostly oxidized when Ni/rGO lost the protection of hydrazine hydrate to expose in the air. According to the above results analysis, metal Ni nanoparticles modified rGO were successfully

prepared.

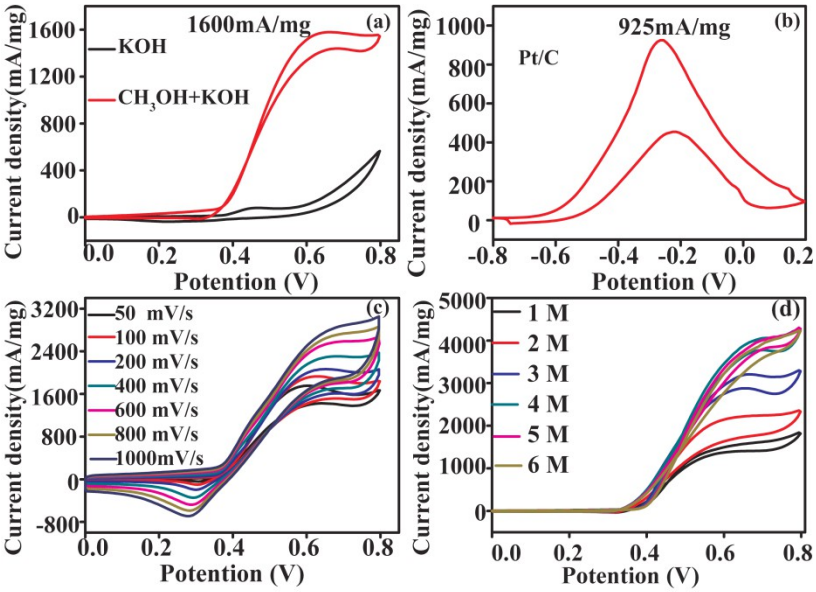

Figure 2 (a) CV curves of the prepared Ni/rGO catalysts in 1 M KOH with/without 1 M CH_3OH at a scan rate of 50 mV/s. (b) CV curves of the commercial Pt/C catalysts in 1 M KOH with 1 M CH_3OH. (c) CV curves of Ni/rGO in 1 M KOH with 1 M CH_3OH at different scan rate. (d) CV curves of Ni/rGO at different concentration of methanol (scan rate: 50 mV/s).

The electrocatalytic activity of the prepared Ni/rGO towards methanol oxidation was initially investigated via cyclic voltammetry (CV) in 1 M KOH + 1 M CH_3OH. According to the literature, the electro-oxidation mechanism of methanol on the Ni-based catalyst is according to the followed progress: [12] [36]

$$Ni + 2OH^- \rightarrow Ni(OH)_2 + 2e^- \quad (3)$$

$$Ni(OH)_2 + OH^- \rightarrow NiOOH + H_2O + e^- \quad (4)$$

$$NiOOH + CH_3OH \rightarrow Ni(OH)_2 + \text{oxidation products of methanol} \quad (5)$$

As we can see in equation (5), the formation of NiOOH is the decisive step for electro-oxidation of methanol on Ni-based materials. Thus, before the electrocatalytic activity tests, Ni/rGO catalyst was conditioned by CV over 50 cycles at a scan rate of 50 mV/s in 1 M KOH to enrich hydroxides and oxyhydroxides on the surface of the catalyst, which results in thickening of the electrocatalytic layers.[36] A pair of redox peaks corresponding to the Ni^{2+}/Ni^{3+} redox couple (Figure 2a) is reported to be 0.44 & 0.3V vs Ag/AgCl, respectively.[8] [11] In the presence of 1 M methanol (Figure 2a), an intense anodic peak in the forward scan at 0.6 V suggest the enhanced catalytic

activity for MOR. The ultrahigh mass activity of 1600 mA/mg is not only superior to the previously reported Ni-based catalysts (Table 1), but also higher than that of the commercial Pt/C catalysts (925 mA/mg, Figure 2b). Meanwhile, another minor anodic peak in the reverse scan is attributed to the oxidation of adsorbed intermediate species produced in the forward sweep, indicating the good anti-poisoning properties of Ni/rGO catalyst.[10] [37] Figure 2c shows the effect of scan rate on methanol oxidation at Ni/rGO in 1 M KOH + 1 M CH_3OH. The linear dependence of anodic peak currents on the square root of scan rates (Figure S5a) shows the electrocatalytic reaction as a diffusion controlled process at 1M CH_3OH. Furthermore, Ni/rGO retains the linear growth even at a high scan of 1000 mV/s, which benefits from the ultrafine Ni nanoparticle into on rGO, hollow structure of Ni and the large surface area of rGO, which are benefit for electro species to diffuse efficiently between electrolyte and surface active sites on Ni/rGO.

Table 1 Electrocatalytic performance comparison between Ni/rGO composite and other recently reported Ni-based nanomaterials at a scan rate of 50 mV/s.

Catalysts	Mass activity (mA/mg)	Condition	Ref.
Ni/rGO	1600	1 M CH_3OH+1 M KOH	This work
commercial Pt/C	925	1 M CH_3OH+1 M KOH	This work
Ni-P/RGO	117	0.5 M CH_3OH+1 M KOH	31
nanosphere-like $NiCo_2O_4$	40.9	0.5 M CH_3OH + 1 M KOH	5
Ni@CNT	966	1 M CH_3OH + 1 M KOH	32
CNFs-Ni	400	0.5 M CH_3OH +1 M KOH	13
CNT-Ni/SiC-700	1000	1 M CH_3OH +1 M KOH	36
Ni-Co-P-O	1567	1 M CH_3OH + 0.5 M KOH	37
microsphere Ni-P	1490	1 M CH_3OH + 0.5 M KOH	11

Apart from the catalytic mass activity, the concentration of methanol is another index to determine the performance of MOR. As high concentration methanol solution could dramatically decrease the size of the fuel cell and simultaneously increase the power density.[38] Unfortunately, most of the preceding Ni-based catalysts have been reported use lower concentrations of methanol such as 0.5 M to 2 M methanol. [37] [36] [13] Interestingly, in the present study, the peak current density increases linearly with methanol concentration up to 4 M (Figure 2d and Figure S5b), indicating the diffusion of reaction species is the rate-limiting step. When the methanol concentration exceed this limit, the oxidation current density keep constant demonstrating the rate-limiting step is changed to a reaction-kinetics-controlled process and its rate are mainly determined by the

catalytic reaction rate of the electrode. The prepared Ni/rGO catalysts exhibit saturation concentration of methanol up to 4 M, which is the highest concentration ever to be reported, especially for Ni-based catalysts for methanol electro-oxidation.

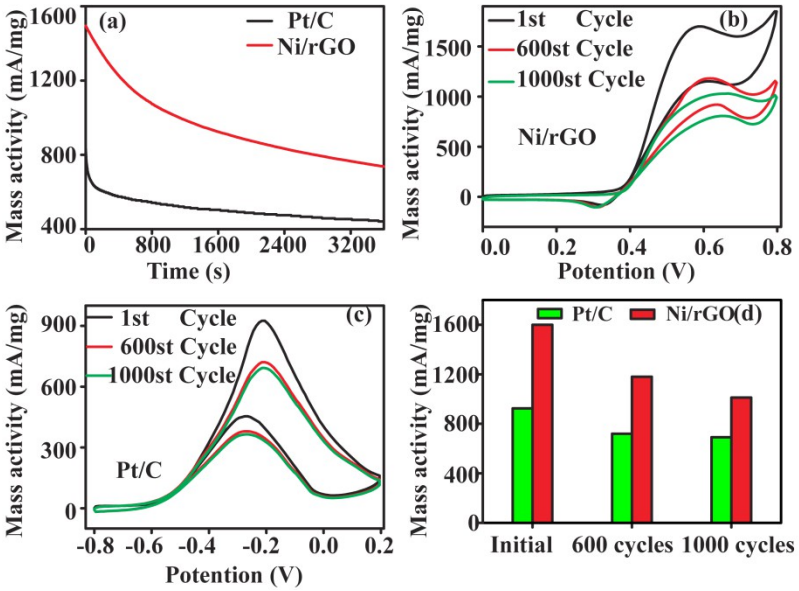

Figure 3 (a) CA plots of Ni/rGO catalysts at 0.6 V and commercial Pt/C catalysts at -0.2V in 1 M KOH with 1M CH_3OH. CV curves of (b) Ni/rGO and (c) commercial Pt/C catalysts in 1 M KOH with 1 M CH_3OH at different cycles (scan rate: 50mV/s). (d) Catalytic mass activity of Ni/rGO and commercial Pt/C catalysts at different cycles.

To evaluate the electrochemical stability, the chronoamperometry (CA) tests and cycling test of the prepared Ni/rGO and commercial Pt/C catalysts were carried out in 1 M KOH solution with 1 M CH_3OH. Figure 3a shows the CA curves for methanol of Ni/rGO catalyst at 0.6 V and the commercial Pt/C catalyst at -0.22V for 3600 s. The Ni/rGO catalyst maintains obviously higher current densities than commercial Pt/C catalyst during the whole test, indicating a higher poison-tolerance to absorbed intermediates generated during the methanol oxidation processes.[10] Figure 3b, c show CV curves of the Ni/rGO composite and commercial Pt/C catalysts at different cycles respectively. Although the decay of the mass activity of the Ni/rGO composite (67.2 %) is much faster than that of Pt/C (74.81%), the Ni/rGO composite maintain super mass activity of 1012 mA/mg even after 1000 cycles whereas that of Pt/C just keep 692 mA/mg (Figure 3d). The TEM images of the Ni/rGO after cycling tests (Fig. S7, ESI†) show that the Ni nanoparticles keep the original morphology and free of agglomeration, indicating that the active site of Ni is stable during

the reaction process and successfully explain its outstanding durability.

Generally speaking, the prepared Ni/rGO is a superior catalytic for methanol with high mass activity of 1600 mA/mg, good anti-poisoning properties, fast reaction kinetics and high saturation concentration of methanol. The superior catalytic performances result from the unique structure and high dispersity of Ni nanoparticles on rGO (TEM images (Fig. 1e-g), which provide abundant the reaction sites for the oxidation of methanol promoting the complete oxidation of methanol.[39] Moreover, some ultrafine Ni nanoparticles with the size of 1.5-3.6 nm are embedded into rGO and converted to the active site NiOOH anchoring on the surface of rGO, which prevent Ni nanoparticles from aggregation during the reaction. Furthermore, the excellent mass and electron transportation performance of rGO would like to diffuse fast between electrolyte and surface active sites on Ni/rGO to facilitate the operation of the reaction. As a result, the Ni/rGO catalyst exhibit excellent performance for the electro-oxidation of methanol.

Conclusions

In this work, we fabricated Ni/rGO catalysts as a highly efficient toward MOR in alkaline condition. The obtained Ni/rGO exhibited an impressively high electrocatalytic activity, good anti-poisoning properties, fast reaction kinetics and high concentration of methanol (4 M). The super performance could be attributed to the unique structures of Ni nanoparticles especially the ultrafine Ni nanoparticles (1.5 nm - 3.6 nm), stable structure during the reaction and the excellent electron transportation of rGO. The facile, cost-effectiveness preparation of non-noble metal/graphene with the high activity is significant for the sustainable development.

Acknowledgement

We thank the financial supports from the National Basic Research Program of China (2014CB931704), the National Natural Science Foundation of China (NSFC, No. 11304315, 11204308, 51401206, 11404338, 51371166) and the CAS/SAFEA International Partnership Program for Creative Research Teams).

References

1. Fu, X. Z.; Liang, Y.; Chen, S. P.; Lin, J. D.; Liao, D. W., Pt-rich shell coated Ni nanoparticles as catalysts for methanol electro-oxidation in alkaline media. *Catalysis Communications* **2009,** *10* (14), 1893-1897.

2. Xie, S.; Tong, X. L.; Jin, G. Q.; Qin, Y.; Guo, X. Y., CNT-Ni/SiC hierarchical nanostructures: preparation and their application in electrocatalytic oxidation of methanol. *Journal of Materials*

Chemistry A **2013,** *1* (6), 2104-2109.

3. (a) Wu, S. L.; Liu, J.; Liang, D. W.; Sun, H. M.; Ye, Y. X.; Tian, Z. F.; Liang, C. H., Photo-excited in situ loading of Pt clusters onto rGO immobilized SnO2 with excellent catalytic performance toward methanol oxidation. *Nano Energy* **2016,** *26*, 699-707; (b) Dai, L.-X.; Wang, X.-Y.; Zheng, X.-Y.; Zhang, Y.-W., Pt and Pt-Rh supercrystals self-assembled in N,N-dimethylformamide. *Chemical communications* **2016,** *52* (28), 5023-5026.

4. Liang, X.; Liu, B.; Zhang, J.; Lu, S.; Zhuang, Z., Ternary Pd-Ni-P hybrid electrocatalysts derived from Pd-Ni core-shell nanoparticles with enhanced formic acid oxidation activity. *Chemical communications* **2016,** *52* (74), 11143-11146.

5. Gu, L.; Qian, L.; Lei, Y.; Wang, Y.; Li, J.; Yuan, H.; Xiao, D., Microwave-assisted synthesis of nanosphere-like NiCo2O4 consisting of porous nanosheets and its application in electro-catalytic oxidation of methanol. *Journal of Power Sources* **2014,** *261*, 317-323.

6. Gonzalez-Fuentes, M. A.; Manriquez, J.; Gutierrez-Granados, S.; Alatorre-Ordaz, A.; Godinez, L. A., Ni(II) 1,4,8,11-tetraazacyclotetradecane electrocatalytic films prepared on top of surface anchored PAMAM dendrimer layers. A new type of electrocatalytic material for the electrochemical oxidation of methanol. *Chemical communications* **2005,** (7), 898-900.

7. Abdel Rahim, M. A.; Abdel Hameed, R. M.; Khalil, M. W., Nickel as a catalyst for the electro-oxidation of methanol in alkaline medium. *Journal of Power Sources* **2004,** *134* (2), 160-169.

8. Ali Shah, A.-u.-H.; Yasmeen, N.; Rahman, G.; Bilal, S., High Electrocatalytic Behaviour of Ni Impregnated Conducting Polymer Coated Platinum and Graphite Electrodes for Electrooxidation of Methanol. *Electrochimica Acta* **2017,** *224*, 468-474.

9. Gu, C. D.; Huang, M. L.; Ge, X.; Zheng, H.; Wang, X. L.; Tu, J. P., NiO electrode for methanol electro-oxidation: Mesoporous vs. nanoparticulate. *International Journal of Hydrogen Energy* **2014,** *39* (21), 10892-10901.

10. Wang, L.; Zhang, G.; Liu, Y.; Li, W.; Lu, W.; Huang, H., *Nanoscale* **2016,** *8* (21), 11256-63.

11. Tong, Y. Y.; Gu, C. D.; Zhang, J. L.; Huang, M. L.; Tang, H.; Wang, X. L.; Tu, J. P., Three-dimensional astrocyte-network Ni–P–O compound with superior electrocatalytic activity and stability for methanol oxidation in alkaline environments. *J. Mater. Chem. A* **2015,** *3* (8), 4669-4678.

12. Tong, X.; Qin, Y.; Guo, X.; Moutanabbir, O.; Ao, X.; Pippel, E.; Zhang, L.; Knez, M., Enhanced Catalytic Activity for Methanol Electro-oxidation of Uniformly Dispersed Nickel Oxide Nanoparticles-Carbon Nanotube Hybrid Materials. *Small* **2012,** *8* (22), 3390-3395.

13. Wang, J.; Zhao, Q.; Hou, H.; Wu, Y.; Yu, W.; Ji, X.; Shao, L., Nickel nanoparticles supported on nitrogen-doped honeycomb-like carbon frameworks for effective methanol oxidation. *RSC Adv.* **2017,** *7* (23), 14152-14158.

14. Das, S.; Dutta, K.; Kundu, P. P., Nickel nanocatalysts supported on sulfonated polyaniline: potential toward methanol oxidation and as anode materials for DMFCs. *J. Mater. Chem. A* **2015,** *3* (21), 11349-11357.

15. Liao, Y.; Pan, S.; Bian, C.; Meng, X.; Xiao, F.-S., Improved catalytic activity in methanol electro-oxidation over the nickel form of aluminum-rich beta-SDS zeolite modified electrode. *Journal of Materials Chemistry A* **2015,** *3* (11), 5811-5814.

16. Bhowmik, K.; Mukherjee, A.; Mishra, M. K.; De, G., Stable Ni nanoparticle-reduced graphene oxide composites for the reduction of highly toxic aqueous Cr(VI) at room temperature. *Langmuir : the ACS journal of surfaces and colloids* **2014,** *30* (11), 3209-16.

17. Li, L.; Wu, Y.; Lu, J.; Nan, C.; Li, Y., Synthesis of Pt-Ni/graphene via in situ reduction and its

enhanced catalyst activity for methanol oxidation. *Chemical communications* **2013,** *49* (68), 7486-7488.

18. Lv, L.-B.; Ye, T.-N.; Gong, L.-H.; Wang, K.-X.; Su, J.; Li, X.-H.; Chen, J.-S., Anchoring Cobalt Nanocrystals through the Plane of Graphene: Highly Integrated Electrocatalyst for Oxygen Reduction Reaction. *Chemistry of Materials* **2015,** *27* (2), 544-549.

19. Wu, Y.-g.; Wen, M.; Wu, Q.-s.; Fang, H., Ni/graphene Nanostructure and Its Electron-Enhanced Catalytic Action for Hydrogenation Reaction of Nitrophenol. *The Journal of Physical Chemistry C* **2014,** *118* (12), 6307-6313.

20. Qin, Y.; Chao, L.; Yuan, J.; Liu, Y.; Chu, F.; Kong, Y.; Tao, Y.; Liu, M., Ultrafine Pt nanoparticle-decorated robust 3D N-doped porous graphene as an enhanced electrocatalyst for methanol oxidation. *Chemical communications* **2016,** *52* (2), 382-385.

21. Chen, G.; Wang, F.; Liu, F.; Zhang, X., One-pot preparation of Ni-graphene hybrids with enhanced catalytic performance. *Applied Surface Science* **2014,** *316*, 568-574.

22. Neiva, E. G.; Souza, V. H.; Huang, K.; Penicaud, A.; Zarbin, A. J., Graphene/nickel nanoparticles composites from graphenide solutions. *Journal of colloid and interface science* **2015,** *453*, 28-35.

23. Zhang Peng, Z. Z., Dyatkin Boris, Liu Chang and Qiu Jieshan, In situ synthesis of cotton-derived Ni/C catalysts with controllable structures and enhanced catalytic performance. *Green Chemistry* **2016,** *18*, 3594-3599.

24. Ye, Y.; Wang, P.; Dai, E.; Liu, J.; Tian, Z.; Liang, C.; Shao, G., A novel reduction approach to fabricate quantum-sized SnO(2)-conjugated reduced graphene oxide nanocomposites as non-enzymatic glucose sensors. *Physical chemistry chemical physics : PCCP* **2014,** *16* (19), 8801-7.

25. Wu, S. L.; Liu, J.; Tian, Z. F.; Cai, Y. Y.; Ye, Y. X.; Yuan, Q. L.; Liang, C. H., Highly Dispersed Ultrafine Pt Nanoparticles on Reduced Graphene Oxide Nanosheets: In Situ Sacrificial Template Synthesis and Superior Electrocatalytic Performance for Methanol Oxidation. *Acs Appl Mater Inter* **2015,** *7* (41), 22935-22940.

26. Marcano, D. C.; Kosynkin, D. V.; Berlin, J. M.; Sinitskii, A.; Sun, Z. Z.; Slesarev, A.; Alemany, L. B.; Lu, W.; Tour, J. M., Improved Synthesis of Graphene Oxide. *Acs Nano* **2010,** *4* (8), 4806-4814.

27. Hummers, W. S., Jr; Offeman, R. E. , Preparation of Graphitic Oxide. *J. Am. Chem. Soc.* **1958,** *80*, 1339.

28. Zhang, H. M.; Liu, J.; Ye, Y. X.; Tian, Z. F.; Liang, C. H., Synthesis of Mn-doped alpha-Ni(OH)(2) nanosheets assisted by liquid-phase laser ablation and their electrochemical properties. *Phys Chem Chem Phys* **2013,** *15* (15), 5684-5690.

29. Muñetón Arboleda, D.; Santillán, J. M. J.; Mendoza Herrera, L. J.; van Raap, M. B. F.; Mendoza Zélis, P.; Muraca, D.; Schinca, D. C.; Scaffardi, L. B., Synthesis of Ni Nanoparticles by Femtosecond Laser Ablation in Liquids: Structure and Sizing. *The Journal of Physical Chemistry C* **2015,** *119* (23), 13184-13193.

30. Jung, H. J.; Choi, M. Y., Specific Solvent Produces Specific Phase Ni Nanoparticles: A Pulsed Laser Ablation in Solvents. *The Journal of Physical Chemistry C* **2014,** *118* (26), 14647-14654.

31. (a) Wang, D.-P.; Sun, D.-B.; Yu, H.-Y.; Meng, H.-M., Morphology controllable synthesis of nickel nanopowders by chemical reduction process. *Journal of Crystal Growth* **2008,** *310* (6), 1195-1201; (b) Wang, D. P.; Sun, D. B.; Yu, H. Y.; Meng, H. M., Morphology controllable synthesis of nickel nanopowders by chemical reduction process. *Journal of Crystal Growth* **2008,** *310* (6), 1195-1201.

32. Zhang, W.; Li, Y.; Peng, S., Template-free synthesis of hollow Ni/reduced graphene oxide composite for efficient H2 evolution. *J. Mater. Chem. A* **2017**.

33. Beate Ritz; Hauke Heller; Santiago Melchor; Anton Myalitsin; Jose A. Dobado; Andreas Kornowski; * Beatriz H. Jua´ rez; Horst Weller; Francisco J. Martin-Martinez; Klinke†, a. C., Reversible Attachment of Platinum Alloy Nanoparticles to Nonfunctionalized Carbon Nanotubes. *ACS Nano* **2010,** *4* (4), 2438-2444.

34. Zhang, H.; Gu, C.-D.; Huang, M.-L.; Wang, X.-L.; Tu, J.-P., Anchoring three-dimensional network structured Ni–P nanowires on reduced graphene oxide and their enhanced electrocatalytic activity towards methanol oxidation. *Electrochemistry Communications* **2013,** *35*, 108-111.

35. Wu, S.; Liu, J.; Tian, Z.; Cai, Y.; Ye, Y.; Yuan, Q.; Liang, C., Highly Dispersed Ultrafine Pt Nanoparticles on Reduced Graphene Oxide Nanosheets: In Situ Sacrificial Template Synthesis and Superior Electrocatalytic Performance for Methanol Oxidation. *ACS Appl Mater Interfaces* **2015,** *7* (41), 22935-40.

36. Wang, J.; Teschner, D.; Yao, Y.; Huang, X.; Willinger, M.; Shao, L.; Schlögl, R., Fabrication of nanoscale NiO/Ni heterostructures as electrocatalysts for efficient methanol oxidation. *J. Mater. Chem. A* **2017,** *5* (20), 9946-9951.

37. Asgari, M.; Maragheh, M. G.; Davarkhah, R.; Lohrasbi, E., Methanol Electrooxidation on the Nickel Oxide Nanoparticles/Multi-Walled Carbon Nanotubes Modified Glassy Carbon Electrode Prepared Using Pulsed Electrodeposition. *Journal of the Electrochemical Society* **2011,** *158* (12), K225-K229.

38. Ko, T. H.; Devarayan, K.; Seo, M. K.; Kim, H. Y.; Kim, B. S., Facile Synthesis of Core/Shell-like NiCo2O4-Decorated MWCNTs and its Excellent Electrocatalytic Activity for Methanol Oxidation. *Scientific Reports* **2016,** *6*.

39. Antolini, E.; Gonzalez, E. R., Alkaline direct alcohol fuel cells. *Journal of Power Sources* **2010,** *195* (11), 3431-3450.